International Journal of Nanomedicine

Dovepress

open access to scientific and medical research

Open Access Full Text Article

ORIGINAL RESEARCH

$CaCO_3$/$CaIP_6$ composite nanoparticles effectively deliver AKT1 small interfering RNA to inhibit human breast cancer growth

This article was published in the following Dove Press journal:
International Journal of Nanomedicine
1 July 2015
Number of times this article has been viewed

Hongyan Zhou[1,*]
Jinhuan Wei[2,*]
Qiangsheng Dai[3]
Liping Wang[4]
Junhang Luo[2]
Tuckyun Cheang[4]
Shenming Wang[4]

[1]Department of Neurological Intensive Care Unit, First Affiliated Hospital, Sun Yat-Sen University, Guangzhou, People's Republic of China; [2]Department of Urology, First Affiliated Hospital, Sun Yat-Sen University, Guangzhou, People's Republic of China; [3]Department of Oncology, First Affiliated Hospital, Sun Yat-Sen University, Guangzhou, People's Republic of China; [4]Department of Breast Surgery, First Affiliated Hospital, Sun Yat-Sen University, Guangzhou, People's Republic of China

*These authors contributed equally to this work

Background: Small interfering RNA (siRNA)-mediated gene therapy is a promising strategy to temporarily inhibit the expression of genes involved in development of breast cancer. The lack of a safe and efficient gene delivery system has become a major hurdle for siRNA-mediated gene therapy in breast cancer. Our previous studies have demonstrated that inorganic amorphous calcium carbonate (ACC) hybrid nanospheres functionalized with $CaIP_6$ (ACC/$CaIP_6$) nanoparticles are an efficient nucleic acid delivery tool. The present study aimed to evaluate the safety and efficiency of ACC/$CaIP_6$ in delivering siRNA targeting AKT1 (siAKT1) for the treatment of breast cancer.

Methods: The cytotoxicity of the ACC/$CaIP_6$ nanoparticles was evaluated using a tetrazolium assay. The transfection efficiency and intracellular distribution of ACC/siAKT1 were analyzed by flow cytometry and confocal laser scanning microscopy, respectively. A series of in vitro and in vivo assays was performed to evaluate the effects of ACC/$CaIP_6$/siAKT1 on growth of breast cancer cells.

Results: ACC/$CaIP_6$ nanoparticles effectively transfected cells with little or no toxicity. AKT1 knockdown by ACC/$CaIP_6$/siAKT1 inhibited cell cycle progression and promoted apoptosis of MCF-7 cells. Intratumoral injection of ACC/$CaIP_6$/siAKT1 significantly suppressed the growth of breast cancer in mice.

Conclusion: ACC/$CaIP_6$ nanoparticles are a safe and efficient method of delivering siRNA for gene therapy in breast cancer.

Keywords: breast cancer, gene therapy, nanoparticles, small interfering RNA

Introduction

Traditional cancer treatment is primarily based on chemical drugs and widely used biological agents. Increased understanding of the pathophysiology behind combined immunodeficiency diseases and cancers has led to the realization that targeting these diseases at a genetic level may change and even reverse disease development. Gene therapy modifies cellular gene expression to treat these diseases, and has the potential to treat gene disorders and provide an alternative to conventional cancer therapies.[1,2] The most critical step in gene therapy is to efficiently and stably deliver the therapeutic gene into the targeted cells or organs without degradation and without causing side effects. The lack of an efficient gene delivery system has been a major hurdle for gene therapy in recent years. An ideal gene delivery system must be specific, biodegradable, nontoxic, nonimmunogenic, and stable in storage.[3]

In the past few decades, both viral and nonviral carriers have been used as potential delivery systems for gene therapies. Viral carriers are able to mediate gene delivery with high efficiency and produce long-term gene expression. However, safety concerns,

Correspondence: Shenming Wang
Department of Breast Surgery, First Affiliated Hospital, Sun Yat-Sen University, Guangzhou, 510080, People's Republic of China
Tel +86 133 0222 4168
Fax +86 20 8775 5766
Email shenmingwang@vip.sohu.com

Tuckyun Cheang
Department of Breast Surgery, First Affiliated Hospital, Sun Yat-Sen University, Guangzhou, 510080, People's Republic of China
Tel +86 136 3132 2559
Fax +86 20 8775 5766
Email 13631322559@163.com

such as acute immune responses and immunogenicity, have been raised in clinical trials of gene therapy. Nonviral carriers, which include cationic polymers, liposomes,[4,5] solid lipid nanoparticles,[6] and inorganic nanoparticles, have shown promise because of their advantages, including lack of immunogenicity, low toxicity, and the potential for tissue specificity.[7,8] Unfortunately, among these nonviral delivery systems, lipid-based gene delivery has the limitations of difficulty forming DNA–liposome complexes and toxicity to some cell types. Poor gene transfer efficiency has limited the clinical application of cationic polymers.[9] Nanoparticles have also been shown to be highly promising platforms for therapeutics.[10]

We have developed a small interfering RNA (siRNA) delivery system comprising inorganic amorphous calcium carbonate (ACC) hybrid nanospheres, functionalized with a Ca(II)-inositol hexakisphosphate compound ($CaIP_6$) composite nanoparticles.[11,12] ACC/$CaIP_6$ nanoparticles can efficiently transfer siRNA into human vascular smooth muscle cells in vitro[12] and into T24 human bladder cancer cells in vivo and in vitro.[11] However, due to the limited number of cell lines tested, the use of ACC/$CaIP_6$ nanoparticles as a gene vector system cannot be generalized. Breast cancer is the second most common cancer in women worldwide.[13] While chemotherapy remains the backbone of current breast cancer treatment, it is limited by a narrow therapeutic index, significant toxicity leading to severe side effects, and the potential for acquired resistance. These obstacles call for novel therapeutic approaches based on various combinations of anticancer drugs and procedures. Nanoparticle-mediated gene therapy is an emergent strategy for breast cancer treatment.[14] On these grounds, the present study was designed to determine whether ACC/$CaIP_6$ nanoparticles exert similar functions in human breast cancer cells and to confirm their potential in gene therapy.

Materials and methods

Cell culture and reagents

MCF-7 human breast tumor cells were obtained from the American Type Culture Collection (Manassas, VA, USA). MCF-7 cells were cultured in Dulbecco's Modified Eagle's Medium (Corning Inc, Tewksbury, MA, USA) with 10% fetal bovine serum (Corning Inc) at 37°C in 5% CO_2. The Lipofectamine 2000 transfection kit (Invitrogen, Carlsbad, CA, USA) was used according to the manufacturer's instructions. Human AKT1-specific siRNA (siAKT1) and control siRNA (siNC) were supplied by Shanghai GenePharma Co, Ltd (Shanghai, People's Republic of China) as follows: AKT1 sense, 5′-UGCCCUUCUACAACCAGGATT-3′; AKT1 antisense, 5′-UCCUGGUUGUAGAAGGGCATT-3′; control sense, 5′-UCCGUUUCGGUCCACAUUCTT-3′; and control antisense, 5′-GAAUGUGGACCGAAACGGATT-3′. Fluorescein-tagged siRNA (FAM-siRNA) was synthesized by modifying the 3′-end of the AKT1 siRNA sense strand. Mouse anti-AKT1 and anti-glyceraldehyde-3-phosphate dehydrogenase were purchased from Abcam (Cambridge, UK).

Gel electrophoresis and cytotoxicity analyses

ACC/$CaIP_6$ nanoparticles and siRNA were mixed at mass ratios of 100:1, 50:1, 30:1, 10:1, or 1:1. The resulting ACC/$CaIP_6$/siRNA mixtures were left at room temperature for 30 minutes to facilitate complexation and then centrifuged at 5,000 rpm for 5 minutes. The suspensions were analyzed by gel electrophoresis at 15 mA for 1 hour using 3% agarose gels prestained with ethidium bromide at a concentration of 0.1 μg/mL. Bands were visualized with an ultraviolet transilluminator.

A 3-(4,5-dimethylthiazol-2-yl)-2,5-diphenyltetrazolium bromide (MTT) assay was used to measure cytotoxicity. MCF-7 cells were seeded at 8×10^3 cells/well in 96-well plates. Cells were then transfected with phosphate-buffered saline (control), siNC alone, siNC with Lipofectamine 2000, or siNC with 10 μg/mL, 50 μg/mL, or 100 μg/mL of ACC/$CaIP_6$ nanoparticles. Treated cells were cultured at 37°C in 5% CO_2 for 4 days. The culture medium was then removed and replaced with 100 μL of fresh medium, and 20 μL of 5 mg/mL MTT was added to each well for 4 hours. The culture medium was again removed, and 150 μL of dimethyl sulfoxide was added. Plates were shaken at 600 rpm for 10 minutes and analyzed at 490 nm.

In vitro transfection and distribution of ACC/$CaIP_6$/FAM-siAKT1

In vitro transfection was performed as previously described.[12] Briefly, cells were trypsinized and seeded at 5×10^4 cells/well in three 24-well plates. The plates were left overnight to achieve 60%–80% confluence, and were then transfected with the predetermined formulations. After 6 hours, cells were analyzed for FAM-siRNA uptake using an inverted fluorescence microscope (IX71, Olympus Corporation, Tokyo, Japan). Cells were also trypsinized, centrifuged (2,000× *g* for 3 minutes), and resuspended in phosphate-buffered saline for flow cytometry analyses (Beckman Coulter, Fullerton, CA, USA).

For confocal laser scanning microscopy, MCF-7 cells were seeded at 5×10^4 cells/well in 35 mm glass bottom

culture dishes (MatTek Corp, Ashland, MA, USA) and then incubated for 24 hours at 37°C in 5% CO_2. Next, the culture medium was replaced with ACC/CaIP$_6$/FAM-siAKT1 complexes in 500 μL of serum-free Dulbecco's Modified Eagle's Medium. Cells were then washed three times with phosphate-buffered saline at predetermined time intervals, and the nuclei were stained with 4′,6′-diamidino-2-phenylinodole (DAPI, Sigma-Aldrich, St Louis, MO, USA) for 5 minutes. The cells were directly observed using an Olympus FluoView confocal microscope and analyzed by FV10-ASW viewer software.

AKT1 expression

MCF-7 cells were seeded at 5×10^4 cells/well in 24-well plates and incubated at 37°C in 5% CO_2 for 24 hours to reach 70% confluence. ACC/CaIP$_6$/siAKT1 (50 nM, 100 nM, or 150 nM siAKT1, 50:1 mass ratio), unloaded ACC/CaIP$_6$, ACC/CaIP$_6$/siNC (150 nM siNC), or phosphate-buffered saline was added to the wells, and the cells were incubated for 24 (mRNA isolation) or 48 (protein extraction) hours.

AKT1 mRNA expression was analyzed by real-time polymerase chain reaction (PCR). Total RNA was extracted with TRIzol reagent (Invitrogen), and complementary DNA was synthesized with the PrimeScript RT Reagent kit (Promega, Madison, WI, USA). Real-time PCR was conducted using an ABI 7900HT fast real-time PCR system (Applied Biosystems, Foster City, CA, USA). Amplification consisted of 30 cycles of 30 seconds at 94°C, 30 seconds at 55°C, and 60 seconds at 72°C. Real-time PCR primers were as follows: human AKT1, forward: 5′-ATGAGCGACGTGGCTATTGTGAAG-3′ and reverse: 5′-GAGGCCGTCAGCCACAGTCTGGATG-3′; and glyceraldehyde-3-phosphate dehydrogenase, forward: 5′-CCCACATGGCCTCCAAGGAGTA-3′ and reverse: 5′-GTGTACATGGCAACTGTGAGGAGG-3′.

For Western blot analyses, equal amounts of whole cell lysates were resolved by sodium dodecyl sulfate polyacrylamide gel electrophoresis and transferred to polyvinylidene difluoride membranes (Pall Corp, Port Washington, NY, USA). Membranes were then incubated at room temperature for 1 hour each with primary and then secondary mouse monoclonal antibodies (5% milk in Phosphate-buffered saline with Tween 20). Immunoreactive proteins were detected with enhanced chemiluminescence detection reagents (Amersham Biosciences, Uppsala, Sweden), according to the manufacturer's instructions.

Cell proliferation, apoptosis, and cell cycle analyses

Cell proliferation after siAKT1 transfection was determined using the MTT assay. MCF-7 cells were seeded at 8×10^3 cells/well in 96-well plates and then treated with the various ACC/CaIP$_6$/siRNA formulations for 24, 48, 72, 96, 120, and 144 hours. Next, 20 μL of MTT (Sigma-Aldrich) solution (5 mg/mL) was added to each well, and cells were incubated for 4 hours. The reaction was stopped by drawing off all medium and adding 150 μL of dimethyl sulfoxide. Optical density was measured at 490 nm with a microplate spectrophotometer.

To analyze apoptosis, MCF-7 cells were seeded at 5×10^4 cells/well in 24-well plates. MCF-7 cells were transfected with the different ACC/CaIP$_6$/siRNA formulations and then stained 48 hours post-transfection using the Annexin V-PE (phycoerythrin) apoptosis detection kit (BD Biosciences, San Jose, CA, USA). The percentage of apoptotic cells was quantified by flow cytometry; viable cells were both negative for Annexin V-PE and propidium iodide.

To analyze cell cycles, MCF-7 cells were seeded at 5×10^4 cells/well in 24-well plates and transfected with ACC/CaIP$_6$/siAKT1, ACC/CaIP$_6$/siNC, unloaded ACC/CaIP$_6$NPs, or phosphate-buffered saline. After 48 hours, each well was trypsinized, and the cells were fixed using 70% ethanol. Cells were stained using the Coulter DNA-Prep Reagents kit (Beckman Coulter), and the cellular DNA content from each sample was determined by flow cytometry (Becton Dickinson, San Jose, CA, USA). All experiments were performed in triplicate.

Tumor suppression in vivo

BALB/c nu/nu immunodeficient mice (6 weeks old, 18–20 g) were purchased from Shanghai Slac Laboratory Animal Co, Ltd (Shanghai, People's Republic of China). Mice were subcutaneously injected in the dorsal flank with 4×10^7 MCF-7 cells in 100 μL of phosphate-buffered saline using a 25-gauge needle. Once the MCF-7 cells developed into tumors (tumor volume approximately 100 mm^3), the mice were randomized into four treatment groups (n=7 per group): ACC/CaIP$_6$/siAKT1 (20 μg of siAKT1 per injection, 50:1 mass ratio), an equivalent amount of unloaded ACC/CaIP$_6$, siAKT1 only, or phosphate-buffered saline. The treatments were injected directly into the tumors and were repeated every week for a total of five treatments. The long and short axial tumor lengths were measured every other day. The Institute Research Medical Ethics Committee of Sun Yat-Sen University approved this study.

Statistical analyses

All experiments were repeated at least three times. The data are presented as the mean ± standard deviation. The Student's

t-test was used to compare two groups. If more than two groups were compared, one-way analysis of variance followed by Bonferroni's post hoc test was used. A *P*-value <0.05 was considered to be statistically significant.

Results and discussion

Preparation and characterization of ACC/CaIP$_6$ nanoparticles

The detailed methods for preparing the ACC/CaIP$_6$ nanoparticles can be found in our previous studies.[11,12] The nanoparticles were characterized by scanning electron microscopy (Figure 1). Scanning electron micrographs of hybrid ACC/CaIP$_6$ nanoparticles show spherical particles with diameters of 80–200 nm that were composed of approximately 90% ACC and 10% CaIP$_6$. The 80–200 nm sizes and spherical characteristics provide the nanoparticles with a large surface area and a high capacity for surface DNA complexation. The cationic charge (+30.81 mV by zeta potential measurements) of these nanoparticles adsorbed easily on the negatively charged cell membrane surface and consequently afforded the nanoparticles a high likelihood for internalization.[11,12]

ACC/CaIP$_6$ nanoparticle siRNA-binding efficiency, and cytotoxicity in MCF-7 cells

A gel electrophoresis shift assay was performed to confirm ACC/CaIP$_6$/siRNA complexation (Figure 2A). When ACC/CaIP$_6$ and siRNA were present at a mass ratio of 50:1 or greater, the siRNA was completely incorporated into the ACC/CaIP$_6$ nanoparticle complex. These results suggest that the optimal mass ratio for ACC/CaIP$_6$ and siRNA was 50–100 nanoparticles per siRNA (ie, 50–100:1). This is consistent with our previous findings.[11,12]

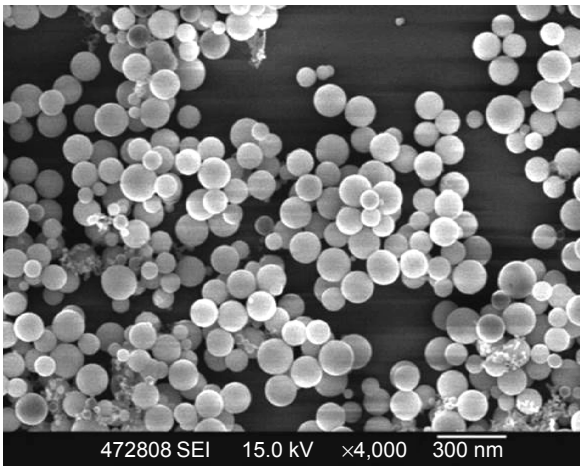

Figure 1 Scanning electron micrograph of amorphous calcium carbonate hybrid nanospheres functionalized with a Ca(II)-inositol hexakisphosphate compound.

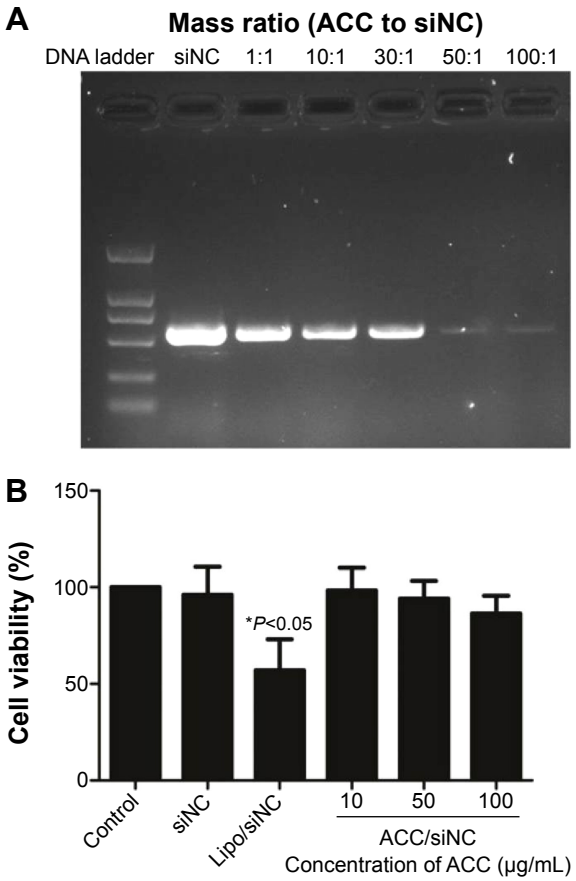

Figure 2 ACC/CaIP$_6$ nanoparticle siRNA-binding efficiency and cytotoxicity in MCF-7 cells.

Notes: (**A**) Gel electrophoresis was used to assess ACC/CaIP$_6$ nanoparticles and siRNA binding at different mass ratios. (**B**) Cytotoxicity was measured by the percentage of viable MCF-7 cells present after ACC/CaIP$_6$ treatment, using the MTT assay 48 hours post–transfection. These percentages were calculated in relation to those of untreated controls. The data show the mean ± standard deviation of three independent experiments (*$P<0.05$ by one-way analysis of variance).

Abbreviations: ACC/CaIP$_6$, amorphous calcium carbonate hybrid nanospheres functionalized with a Ca(II)-inositol hexakisphosphate compound; siNC, control small interfering RNA; lipo, Lipofectamine 2000; siRNA, small interfering RNA.

MTT assays were performed to evaluate the cytotoxicity of ACC/CaIP$_6$ nanoparticles to MCF-7 cells using different concentrations of ACC/CaIP$_6$ complexed with control siRNA. ACC/CaIP$_6$ concentrations of 10 μg/mL or higher with siNC did not significantly affect MCF-7 cells (Figure 2B). In contrast, cells transfected with doses of Lipofectamine 2000 with siNC experienced cytotoxic effects. These results indicate that ACC/CaIP$_6$ nanoparticles have no obvious cytotoxicity when complexed with siRNA transfer vectors in MCF-7 human breast cancer cells.

ACC/CaIP$_6$/siRNA transfection efficiency in MCF-7 cells

We analyzed the cellular uptake of ACC/CaIP$_6$/FAM-siRNA complexes to determine the efficiency of ACC/CaIP$_6$ siRNA delivery in MCF-7 cells. FAM-siRNA was observed within

MCF-7 cells after 6 hours of incubation, indicating efficient ACC/CaIP$_6$/siRNA nanoparticle internalization (Figure 3A).

In addition, ACC/CaIP$_6$/siRNA transfection conditions were optimized by adjusting siRNA concentrations (50–200 nM) at a mass ratio of 50:1. MCF-7 cells were incubated with ACC/CaIP$_6$/FAM-siRNA nanoparticles for 6 hours and then analyzed by flow cytometry. The percentage of fluorescent cells (ie, successfully transfected cells) increased with higher FAM-siRNA concentrations (Figure 3B). In addition, using the 150 nM FAM-siRNA in the ACC/CaIP$_6$/siRNA nanoparticle formation had a nearly identical transfection efficiency when compared with

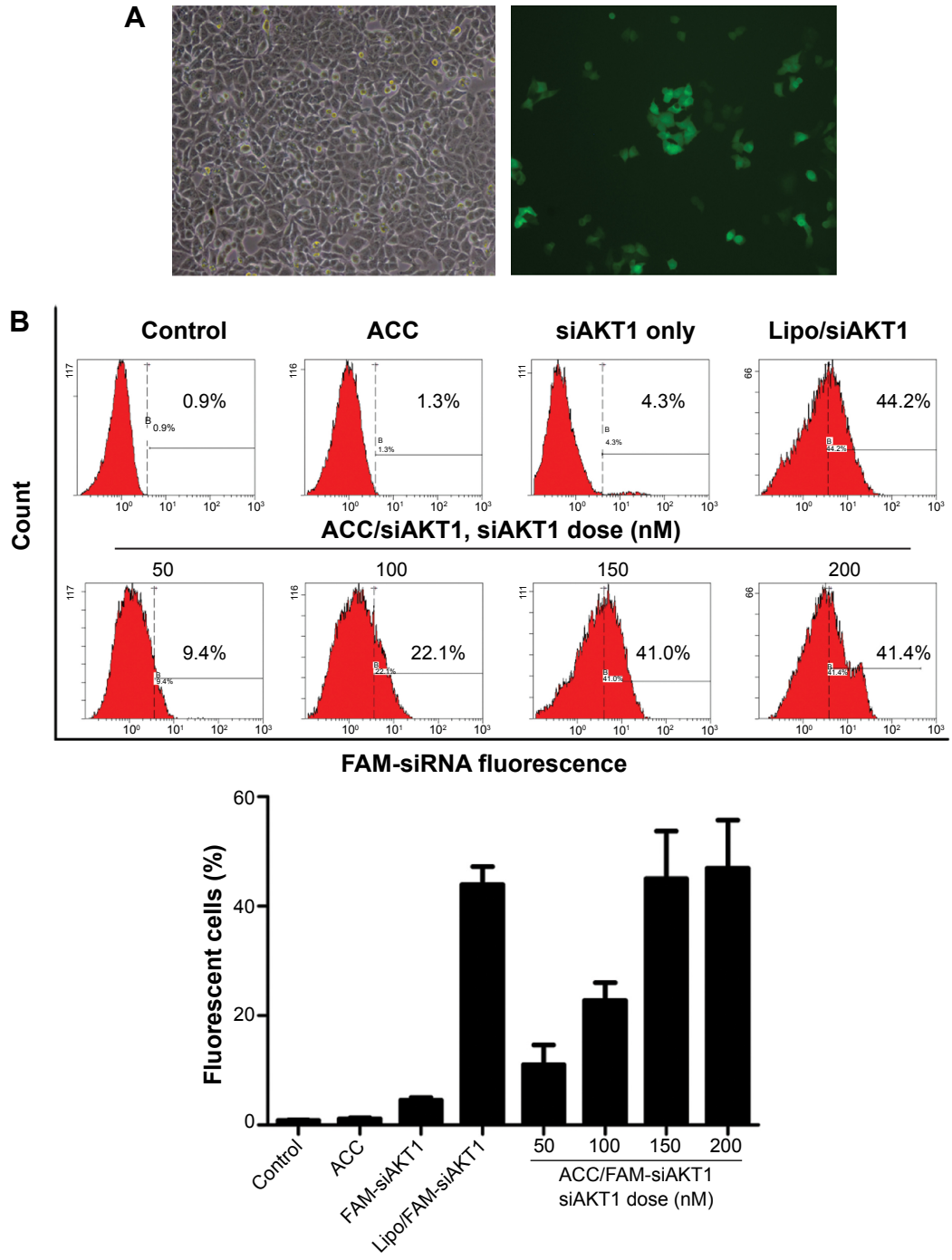

Figure 3 ACC/CaIP$_6$/siRNA transfection efficiency in MCF-7 cells.
Notes: (**A**) Inverted fluorescence microscopy images showing FAM-siRNA fluorescence 6 hours after transfection. (**B**) Representative histograms and percentages (mean ± standard deviation) of fluorescent cells as measured by flow cytometry. The data show the mean ± standard deviation of three independent experiments.
Abbreviations: ACC, amorphous calcium carbonate; ACC/CaIP$_6$, amorphous calcium carbonate hybrid nanospheres functionalized with a Ca(II)-inositol hexakisphosphate compound; FAM-siAKT1, fluorescein-labeled AKT1-specific small interfering RNA; lipo, Lipofectamine 2000.

Lipofectamine 2000/FAM-siRNA. Increasing the FAM-siRNA concentration to 200 nM did not result in an obvious change in transfection efficiency. Therefore, we concluded that the optimal siRNA concentration for ACC/$CaIP_6$ nanoparticle delivery in MCF-7 cells was 150 nM at a mass ratio of 50:1. These values were used in the following experiments.

Intracellular AKT1-specific siRNA distribution in MCF-7 cells

MCF-7 cells were cultured on glass coverslips and incubated with ACC/$CaIP_6$/FAM-siAKT1 complexes to determine whether the nanoparticle complexes could enter the cells. The intracellular distribution of FAM-siAKT1 was observed using confocal laser scanning microscopy. ACC/$CaIP_6$/FAM-siAKT1 complexes (green) were first observed in the MCF-7 cells 1 hour after incubation (Figure 4). At 1 hour, the complexes were mainly distributed at the cell membrane. After 2 hours of incubation, the complexes were distributed in the cytoplasm and along the periphery of the nuclei. FAM-siRNA fluorescence intensity varied considerably, but gradually increased over 8 hours.

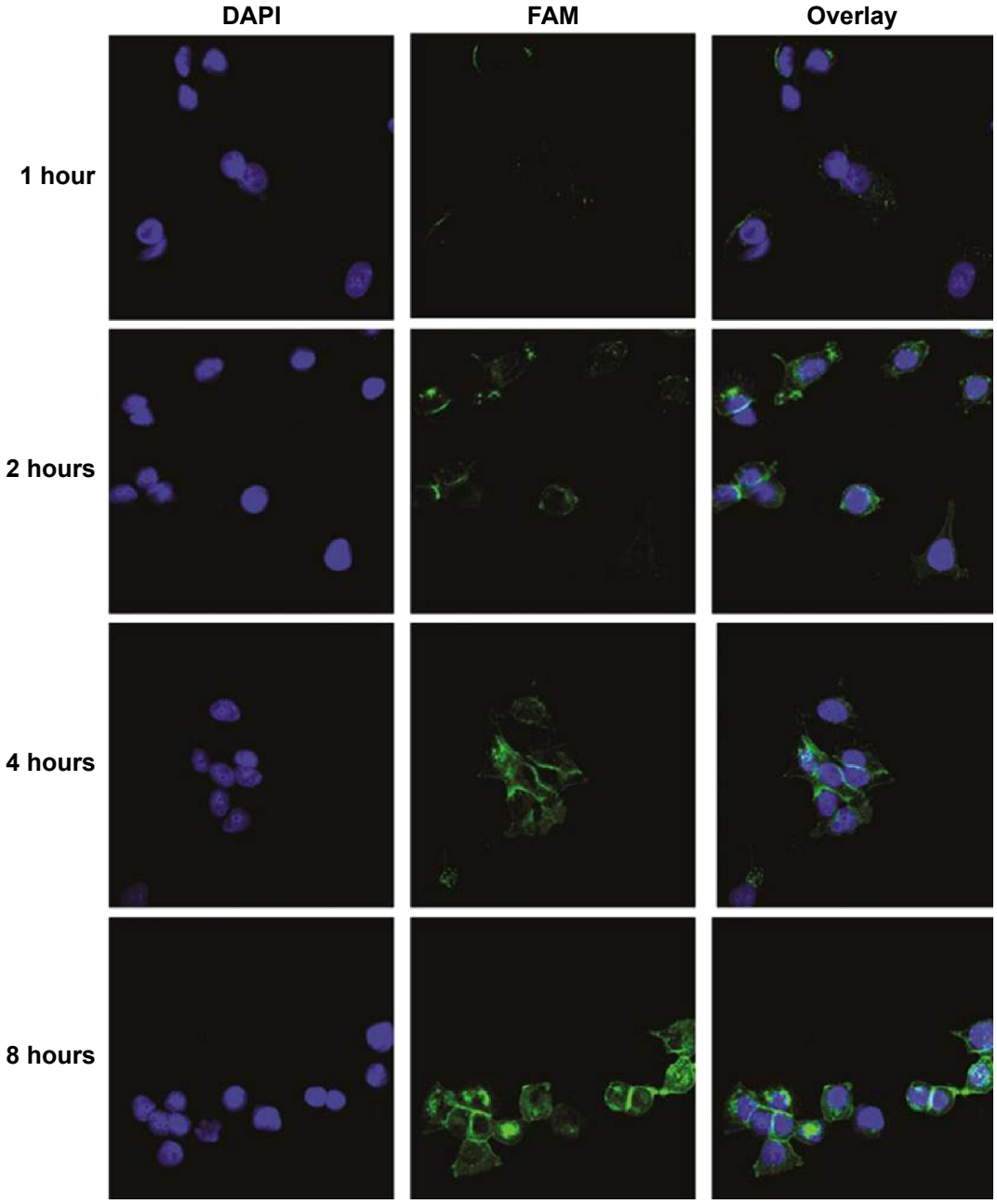

Figure 4 Intracellular siAKT1 distribution in MCF-7 cells.
Notes: FAM-siAKT1 were labeled with fluorescein (green). Cell nuclei were stained with DAPI (blue).
Abbreviations: FAM-siAKT1, fluorescein-labeled AKT1-specific small interfering RNA; DAPI, 4′,6-diamidino-2-phenylindole.

The escape of siRNA from the lysosome after entering the cell is important for subsequent post-transcriptional gene silencing. The hybrid nanoparticles may have resided in endosomes or early lysosomes in the MCF-7 cytoplasm at the beginning of transfection (Figure S1). After 4–8 hours of incubation, FAM-siRNA efficiently escaped from the lysosomal vesicles and exhibited an obvious increase in cytoplasmic fluorescence intensity.

MCF-7 cell growth after knocking down AKT1

Real-time PCR and Western blots were used to measure AKT1 expression and confirm the knockdown of AKT1 following siAKT1 delivery. ACC/CaIP$_6$/siAKT1 nanoparticles efficiently silenced AKT1 expression at both the mRNA and protein levels in MCF-7 cells in an siRNA dose-dependent manner (Figure 5A). This is consistent with the improved transfection efficiency that resulted from increasing the siRNA concentration (Figure 3B). In contrast, the nonloaded nanoparticles did not decrease AKT1 expression in MCF-7 cells.

AKT1, also known as protein kinase B, is a serine/threonine-specific protein kinase that plays a key role in multiple cellular processes, including glucose metabolism, apoptosis, cell proliferation, transcription, and cell migration. To understand the effect of knocking down AKT1 in MCF-7 cells via ACC/CaIP$_6$/siAKT1 transfection, a series of in vitro assays were performed. We used MTT assays to assess MCF-7 cell proliferation after knocking down AKT1. MCF-7 cell growth was significantly inhibited in the ACC/CaIP$_6$/siAKT1 treatment group, and increasing the concentration of siAKT1 enhanced this effect (Figure 5B).

AKT1 affects cell proliferation via signaling cell cycle machinery

Activating AKT1 can overcome G1 and G2 cell cycle arrest,[15,16] and blocking AKT activity with pharmacological or dominant-negative methods leads to cell cycle arrest in certain models.[17,18] AKT has also been shown to play an important role in preventing cyclin D1 degradation.[19] Thus, we examined whether transfecting MCF-7 cells with ACC/CaIP$_6$/siAKT1 complexes affected cell cycle regulation and inhibited cell proliferation.

MCF-7 cells were treated with various nanoparticle and siRNA complexes. The cell cycles of these cells were then analyzed, and the cellular DNA content from each sample was determined by flow cytometry. After incubating with ACC/CaIP$_6$/siAKT1 complexes, the percentage of cells in the G1 phase increased, while the percentage in the S phase decreased (Figure 5C). No such changes were seen in the control groups. Increasing the concentration of siAKT1 in the nanoparticle complexes further decreased the percentage of MCF-7 cells in the S phase. These results suggest that transfecting MCF-7 cells with ACC/CaIP$_6$/siAKT1 complexes in vitro inhibited cell cycle progression and, consequently, cell proliferation.

AKT1 is also involved in cell survival by inhibiting apoptosis. AKT1 inhibits apoptosis by directly phosphorylating several components of the cell death machinery, such as BAD,[20] caspase-9,[21] and FKHR.[22] AKT1 can also influence cell survival by indirectly affecting nuclear factor kappa B[23] and p53.[24] ACC/CaIP$_6$/siAKT1 transfection could exert its antitumor effects by regulating MCF-7 apoptosis. Incubating MCF-7 cells with the ACC/CaIP$_6$/siAKT1 complexes significantly increased cell apoptosis (Figure 5D). In contrast, the ACC/CaIP$_6$ complexes containing siNC were not

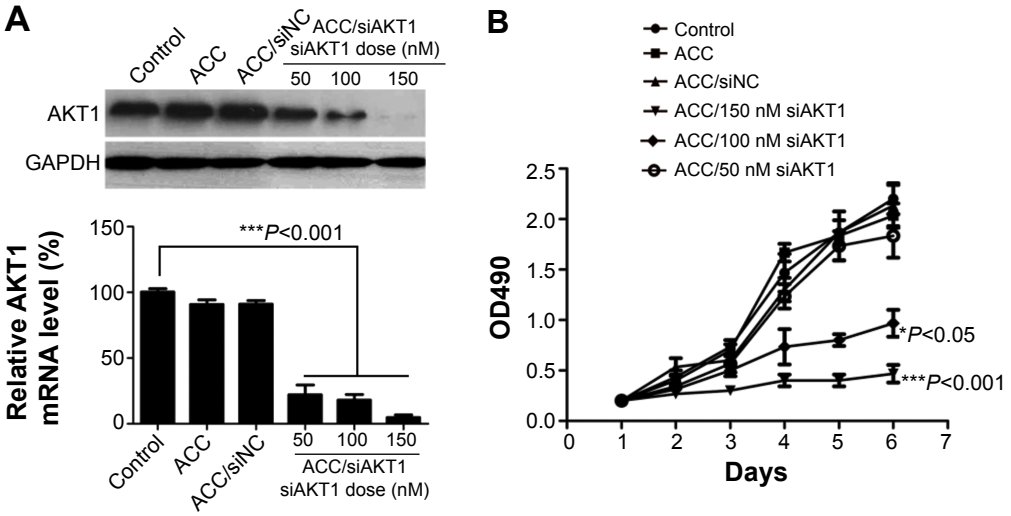

Figure 5 (*Continued*)

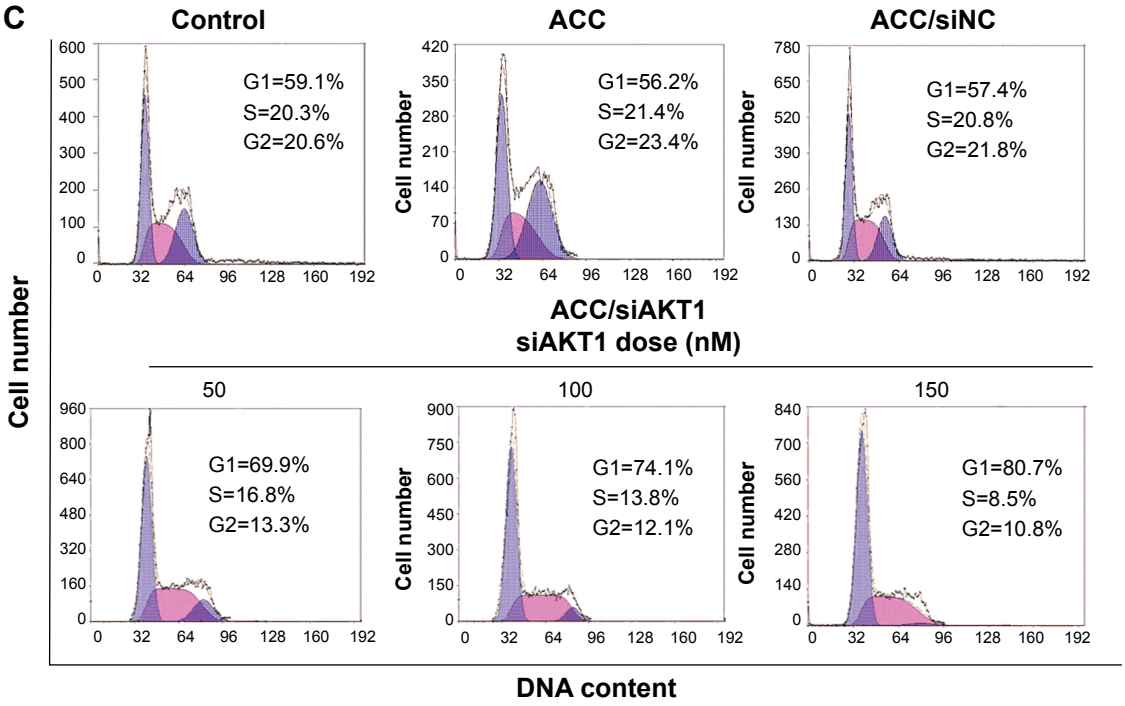

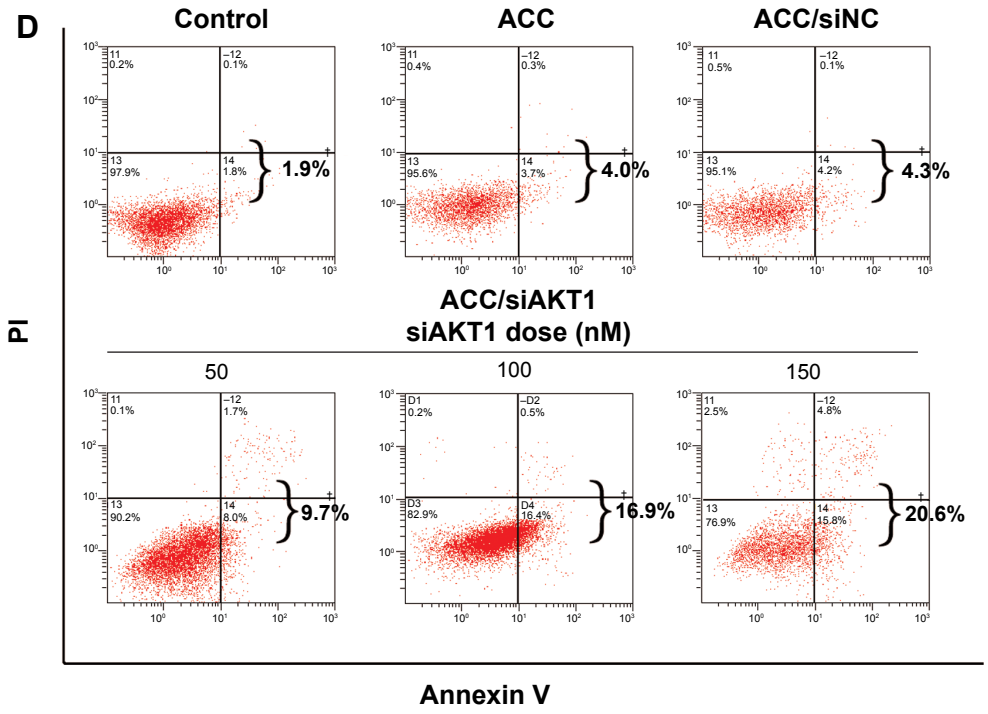

Figure 5 In vitro AKT1 silencing by ACC/CaIP$_6$/siAKT1 transfection in MCF-7 cells.

Notes: (**A**) AKT1 mRNA and protein expression after transfecting MCF-7 cells with ACC/CaIP$_6$/siAKT1 complexes was assessed by real-time polymerase chain reaction and Western blots, respectively. ***$P<0.001$ versus control. (**B**) The MTT assay was used to assess MCF-7 cell viability after transfecting cells with ACC/CaIP$_6$ complexes containing different concentrations of siAKT1 (*$P<0.05$, ***$P<0.001$ versus control). (**C**) Flow cytometry was used to determine the cell cycles of MCF-7 cells 48 hours after ACC/CaIP$_6$/siAKT1 transfection. (**D**) Apoptosis was measured using Annexin V-phycoerythrin/propidium iodide staining for MCF-7 cells treated with various ACC/CaIP$_6$/siRNA complexes (one of three replicates is shown).

Abbreviations: ACC, amorphous calcium carbonate; ACC/CaIP$_6$, amorphous calcium carbonate hybrid nanospheres functionalized with a Ca(II)-inositol hexakisphosphate compound; siAKT1, small interfering AKT1; siNC, control small interfering RNA; OD, optical density; PI, propidium iodide.

significantly different when compared with the control group. These results demonstrate that the observed apoptosis was due to knocking down AKT1 through transfecting MCF-7 cells with ACC/CaIP$_6$/siAKT1 complexes.

Tumor growth after intratumoral injection with ACC/CaIP$_6$/siAKT1 NPs complexes in vivo

The phosphoinositide 3 kinase/Akt/mammalian (or mechanistic) target of the rapamycin (mTOR) pathway is a complicated intracellular pathway, which leads to cell growth and tumor proliferation and plays a significant role in endocrine resistance in breast cancer.[25–27] Increased AKT1 expression and activation has been observed in many human cancers, and is usually caused by upregulation of AKT1 transcription or AKT1 mutations.[28–30] Inhibiting AKT1 is a potential therapeutic strategy for treating these cancers. MK-2206, a novel allosteric AKT1 inhibitor, has been showed to decrease tumor growth and increase murine survival, and is now being tested in clinical trials.[31] Glycerol triacrylate-spermine-mediated delivery of siAKT1 has also been shown to inhibit lung cancer progression.[32]

We performed intratumoral injections of ACC/CaIP$_6$/siAKT1 complexes in mice in order to determine whether

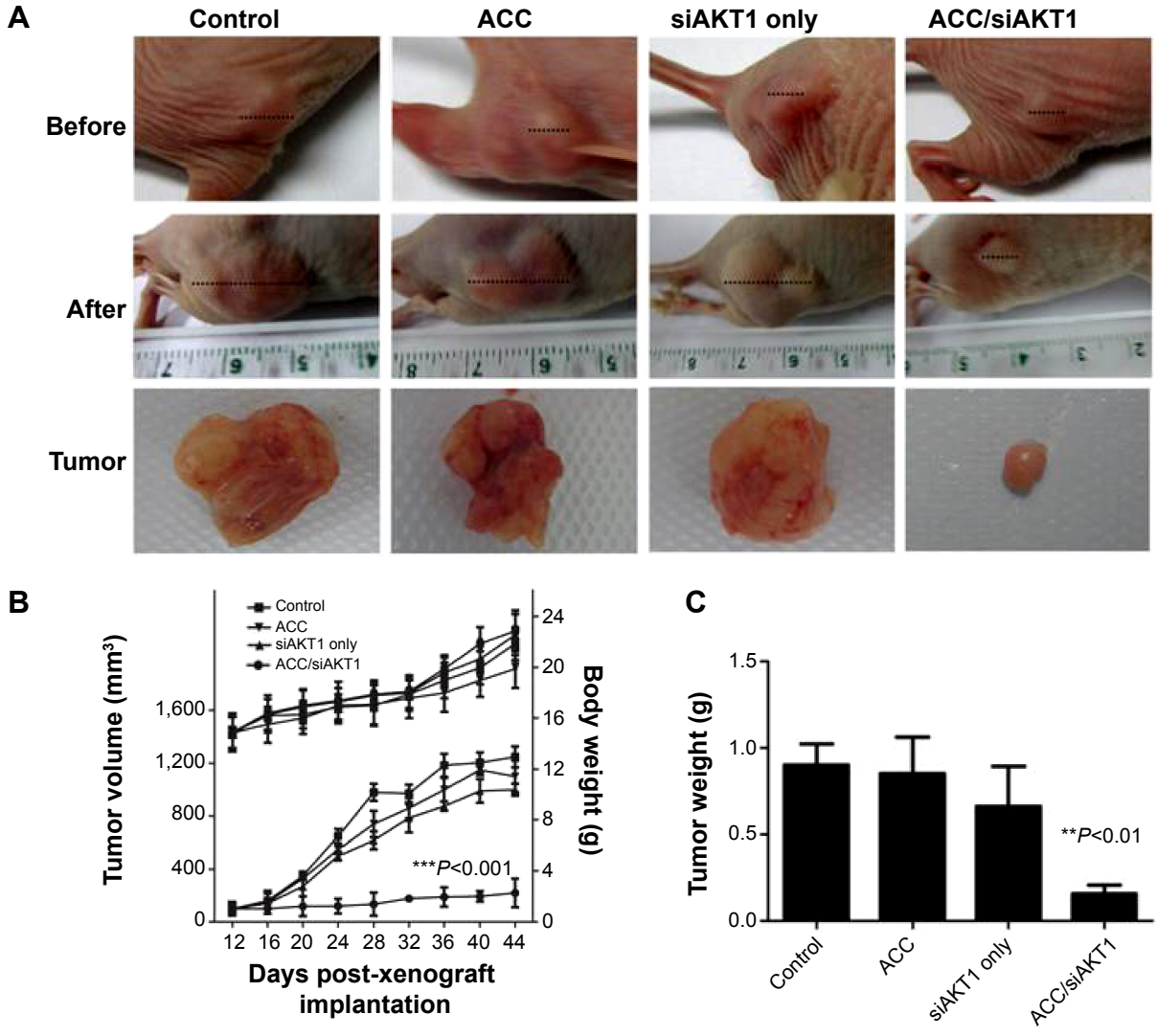

Figure 6 Tumor growth in vivo after intratumoral injections of ACC/CaIP$_6$/siAKT1 nanoparticles.

Notes: (**A**) Representative tumors before and after injection. (**B**) ACC/CaIP$_6$/siAKT1 (20 μg siAKT1/injection, 50:1 mass ratio) was locally injected into the tumors (100 mm^3 in volume at 12 days). Tumor diameter was measured using calipers and tumor volume was calculated using the following formula: volume = $W^2 \times L/2$, where W is the width of the tumor and L is the tumor length. Results are presented as the mean ± standard deviation (n=7 per group; ***$P<0.001$ versus other groups). (**C**) Mean tumor weight (± standard deviation) after mice were sacrificed (n=7 per group; **$P<0.01$ versus other groups).

Abbreviations: ACC, amorphous calcium carbonate; ACC/CaIP$_6$, amorphous calcium carbonate hybrid nanospheres functionalized with a Ca(II)-inositol hexakisphosphate compound; siAKT1, small interfering AKT1.

delivering siAKT1 to MCF-7 tumors with ACC/$CaIP_6$ nanoparticles had therapeutic effects. Athymic mice with MCF-7 xenografts received weekly intratumoral injections of ACC/$CaIP_6$/siAKT1 (20 μg siRNA/injection). Unloaded ACC/$CaIP_6$ nanoparticles and siAKT1 alone were used as negative controls. Real-time quantitative polymerase chain reaction analysis confirmed no significant difference in AKT1 expression in liver samples from each group that had received intratumoral injection with ACC/$CaIP_6$/siAKT1 complexes (Figure S2). Injecting ACC/$CaIP_6$/siAKT1 inhibited tumor growth, while injecting unloaded ACC/$CaIP_6$ nanoparticles or siAKT1 alone did not (Figure 6A and B). Tumor volume did not significantly increase after ACC/$CaIP_6$/siAKT1 treatment, compared with the increased tumor volume observed in the other groups ($P<0.0001$, Figure 6B). These results show that delivering siAKT1 with ACC/$CaIP_6$ nanoparticles inhibited tumor growth. This is also consistent with previous studies on the role of AKT1 in carcinogenesis.[28–31] More importantly, we demonstrate the potential of ACC/$CaIP_6$ nanoparticles for delivering gene vectors in a human breast tumor cell line.

In future studies, we plan to analyze the toxicity and pharmacokinetics of ACC/$CaIP_6$/siRNA nanoparticles when they are administered intravenously. Since specificity is a crucial characteristic of ideal gene therapy delivery, we will also attempt to modify the specificity of these nanoparticles by introducing modifications designed to further enhance transfection efficiency. Furthermore, we will focus on the potential to use this nanocarrier combination therapy.

Conclusion

We have developed ACC/$CaIP_6$ nanoparticles that can efficiently form ACC/$CaIP_6$/siRNA complexes to deliver siRNA into MCF-7 cells. These complexes facilitate the escape of loaded siRNA from the endosome and dissociate from those siRNA, allowing them to specifically downregulate the AKT1 oncogene and, consequently, inhibit cancer cell growth in vitro. Moreover, ACC/$CaIP_6$/siRNA complexes were able to inhibit tumor growth in a murine MCF-7 xenograft model. The present study demonstrates that ACC/$CaIP_6$ nanoparticles are a promising system for effectively delivering siRNA in cancer gene therapy.

Acknowledgment

This work was supported by the National Basic Research Program of China (2010CB934700) and the National Natural Science Foundation of China (30900539, 81172429, 81372821).

Disclosure

The authors report no conflicts of interest in this work.

References

1. Mintzer MA, Simanek EE. Nonviral vectors for gene delivery. *Chem Rev*. 2009;2(109):259–302.
2. Sokolova V, Epple M. Inorganic nanoparticles as carriers of nucleic acids into cells. *Angew Chem Int Ed Engl*. 2008;8(47):1382–1395.
3. Tang F, Hughes JA. Use of disulfide cationic lipids in plasmid DNA delivery. *Methods Mol Med*. 2001;65:79–88.
4. Li W, Szoka FJ. Lipid-based nanoparticles for nucleic acid delivery. *Pharm Res*. 2007;3(24):438–449.
5. Li SD, Huang L. Non-viral is superior to viral gene delivery. *J Control Release*. 2007;3(123):181–183.
6. Del PA, Pujals S, Delgado D, et al. A proline-rich peptide improves cell transfection of solid lipid nanoparticle-based non-viral vectors. *J Control Release*. 2009;1(133):52–59.
7. Davis ME. Non-viral gene delivery systems. *Curr Opin Biotechnol*. 2002;2(13):128–131.
8. Liu C, Zhang N. Nanoparticles in gene therapy principles, prospects, and challenges. *Prog Mol Biol Transl Sci*. 2011;104:509–562.
9. Pack DW, Hoffman AS, Pun S, Stayton PS. Design and development of polymers for gene delivery. *Nat Rev Drug Discov*. 2005;7(4):581–593.
10. Tonga GY, Moyano DF, Kim CS, Rotello VM. Inorganic nanoparticles for therapeutic delivery: trials, tribulations and promise. *Curr Opin Colloid Interface Sci*. 2014;2(19):49–55.
11. Wei J, Cheang T, Tang B, et al. The inhibition of human bladder cancer growth by calcium carbonate/$CaIP_6$ nanocomposite particles delivering AIB1 siRNA. *Biomaterials*. 2013;4(34):1246–1254.
12. Whitehead KA, Langer R, Anderson DG. Knocking down barriers: advances in siRNA delivery. *Nat Rev Drug Discov*. 2009;2(8):129–138.
13. Siegel R, Ma J, Zou Z, Jemal A. Cancer statistics, 2014. *CA Cancer J Clin*. 2014;1(64):9–29.
14. Zadnik PL, Molina CA, Sarabia-Estrada R, et al. Characterization of intratumor magnetic nanoparticle distribution and heating in a rat model of metastatic spine disease. *J Neurosurg Spine*. 2014;6(20):740–750.
15. Kandel ES, Skeen J, Majewski N, et al. Activation of Akt/protein kinase B overcomes a G(2)/m cell cycle checkpoint induced by DNA damage. *Mol Cell Biol*. 2002;22(22):7831–7841.
16. Vemuri GS, Rittenhouse SE. Wortmannin inhibits serum-induced activation of phosphoinositide 3-kinase and proliferation of CHRF-288 cells. *Biochem Biophys Res Commun*. 1994;3(202):1619–1623.
17. Castoria G, Migliaccio A, Bilancio A, et al. PI3-kinase in concert with Src promotes the S-phase entry of oestradiol-stimulated MCF-7 cells. *EMBO J*. 2001;21(20):6050–6059.
18. Diehl JA, Cheng M, Roussel MF, Sherr CJ. Glycogen synthase kinase-3beta regulates cyclin D1 proteolysis and subcellular localization. *Genes Dev*. 1998;22(12):3499–3511.
19. Datta SR, Dudek H, Tao X, et al. Akt phosphorylation of BAD couples survival signals to the cell-intrinsic death machinery. *Cell*. 1997;2(91):231–241.
20. Cardone MH, Roy N, Stennicke HR, et al. Regulation of cell death protease caspase-9 by phosphorylation. *Science*. 1998;5392(282):1318–1321.
21. Brunet A, Bonni A, Zigmond MJ, et al. Akt promotes cell survival by phosphorylating and inhibiting a Forkhead transcription factor. *Cell*. 1999;6(96):857–868.
22. Kane LP, Shapiro VS, Stokoe D, Weiss A. Induction of NF-kappaB by the Akt/PKB kinase. *Curr Biol*. 1999;11(9):601–604.
23. Zhou BP, Liao Y, Xia W, Zou Y, Spohn B, Hung MC. HER-2/neu induces p53 ubiquitination via Akt-mediated MDM2 phosphorylation. *Nat Cell Biol*. 2001;11(3):973–982.

24. Song G, Ouyang G, Bao S. The activation of Akt/PKB signaling pathway and cell survival. *J Cell Mol Med*. 2005;1(9):59–71.
25. Paplomata E, O'Regan R. The PI3K/AKT/mTOR pathway in breast cancer: targets, trials and biomarkers. *Ther Adv Med Oncol*. 2014;4(6):154–166.
26. Ciruelos GE. Targeting the PI3K/AKT/mTOR pathway in estrogen receptor-positive breast cancer. *Cancer Treat Rev*. 2014;7(40):862–871.
27. Cidado J, Park BH. Targeting the PI3K/Akt/mTOR pathway for breast cancer therapy. *J Mammary Gland Biol Neoplasia*. 2012;3–4(17):205–216.
28. Osaki M, Oshimura M, Ito H. PI3K-Akt pathway: its functions and alterations in human cancer. *Apoptosis*. 2004;6(9):667–676.
29. Fresno VJ, Casado E, de Castro J, Cejas P, Belda-Iniesta C, Gonzalez-Baron M. PI3K/Akt signalling pathway and cancer. *Cancer Treat Rev*. 2004;2(30):193–204.
30. Li Z, Yan S, Attayan N, Ramalingam S, Thiele CJ. Combination of an allosteric Akt inhibitor MK-2206 with etoposide or rapamycin enhances the antitumor growth effect in neuroblastoma. *Clin Cancer Res*. 2012;13(18):3603–3615.
31. Hong SH, Kim JE, Kim YK, et al. Suppression of lung cancer progression by biocompatible glycerol triacrylate-spermine-mediated delivery of shAkt1. *Int J Nanomedicine*. 2012;7:2293–2306.
32. Cheang T, Wang S, Hu Z, et al. Calcium carbonate/CaIP$_6$ nanocomposite particles as gene delivery vehicles for human vascular smooth muscle cells. *J Mater Chem.* 2010;20:8050–8055.

Supplementary materials

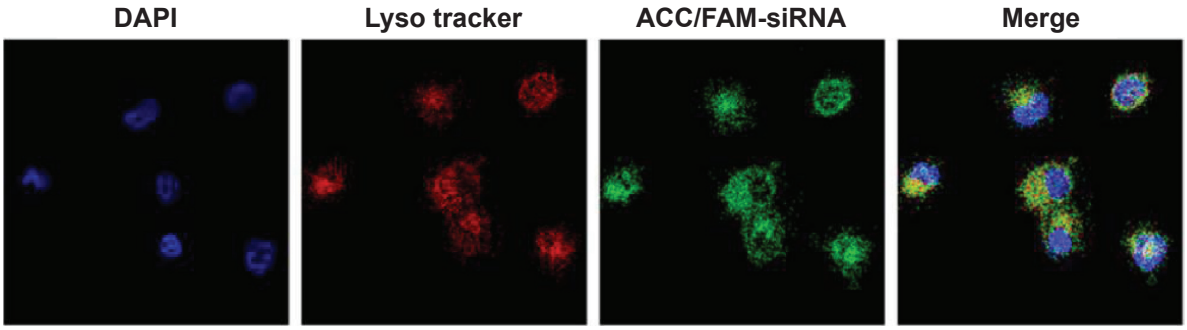

Figure S1 Intracellular distribution of ACC/$CaIP_6$/FAM-siAKT1 in MCF-7 cells was analyzed by confocal laser scanning microscopy after incubation for 8 hours. Lysosomes were stained with Lyso Tracker Red, a percentage of the fluorescence of FAM-siAKT (green) did not overlap with the fluorescence of lysosomes (red), indicating successful escape of the FAM-siRNA from the lysosomes to the cytoplasm.
Abbreviations: ACC/$CaIP_6$, amorphous calcium carbonate hybrid nanospheres functionalized with a Ca(II)-inositol hexakisphosphate compound; FAM-siAKT1, fluorescein-labeled AKT1-specific small interfering RNA.

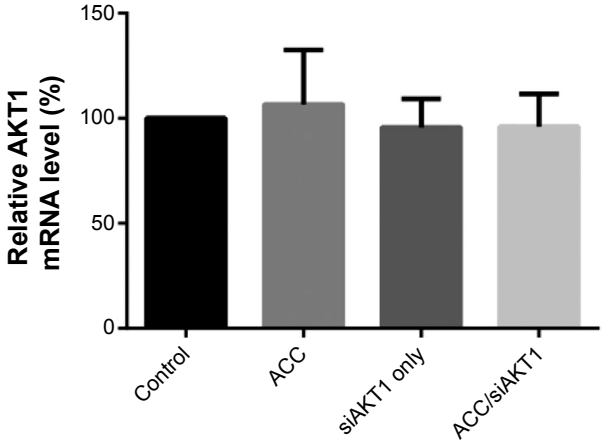

Figure S2 Real-time quantitative polymerase chain reaction analysis of the relative expression of AKT1 mRNA in liver samples intratumorally injected with ACC, siAKT1, and ACC/$CaIP_6$/siAKT1 nanoparticles.
Abbreviations: ACC/$CaIP_6$, amorphous calcium carbonate hybrid nanospheres functionalized with a Ca(II)-inositol hexakisphosphate compound; siAKT1, small interfering AKT1.